Diamond-Based Thin Film Bulk Acoustic Wave Resonator for Biomedical Applications

2013 J. Phys.: Conf. Ser. 477 012009

(http://iopscience.iop.org/1742-6596/477/1/012009)

Diamond-Based Thin Film Bulk Acoustic Wave Resonator for Biomedical Applications

M Zalazar[1] and F Guarnieri[1,2]

[1] Facultad de Ingenieria, Bioingeniera, UNER, Ruta 11 km 10, Oro Verde (3100), Argentina.
[2] CIMEC, INTEC (UNL-CONICET), PTLC, El pozo, Santa Fe (3000), Argentina.

martin.zalazar@fulbrightmail.org

Abstract. Nowadays it is in constant growing the development of thin film bulk acoustic resonators. If the piezoelectric material is going to be implanted in the human body, an important requirement is the biocompatibility of the implant. In this regard, Aluminum Nitride (AlN) has emerged as an attractive alternative for use in biomedical MicroElectroMechanical Systems. Ultrananocrystalline Diamond (UNCD) is a promising material to be used in biomedical applications, due to its extraordinary mulifunctionality; it is exceptional for implantable medical devices requiring stringent biological performance. Since both UNCD and AlN films can be processed via photolithography processes used in microfabrication, the integration of UNCD and AlN films provides the bases for developing a new generation of biocompatible Bio-MEMS/NEMS. Research and development was conducted to produce implantable MEMS devices: Pt/piezoelectric AlN/Pt layer heterostructure was grown and patterned on the UNCD membrane with a Ti adhesion layer. By applying voltages between the top and bottom Pt electrodes layers the piezoelectric AlN layer is energized. The feasibility of the fabrication of biocompatible AlN/diamond-based FBAR structure has been demonstrated.

1. Introduction

Nowadays it is in constant growing the development of thin film bulk acoustic resonator (FBAR). This technology was born as a direct extension of the quartz crystal resonators. These are bulk acoustic wave-based (BAW) thickness mode wave resonators, allowing a reduction in the piezoelectric thickness of the resonator thus conducting to an increased resonance frequency. Therefore, it is reached a high sensibility in gravimetric applications in addition to their compatibility with the integrated circuit technology.

If the piezoelectric material is going to be implanted in the human body, an important requirement is the biocompatibility of the implant. It would be desirable to have a biocompatible piezoelectric material, thus avoiding the need for packaging that represents a significant portion of the cost to the device. In this regard, Aluminum Nitride (AlN) has emerged as an attractive alternative to other piezoelectric materials as have been shown by several authors [1][2]. AlN is a very attractive piezoelectric material for use in biomedical MicroElectroMechanical Systems (BioMEMS); it is biocompatible, exhibits high resistivity, high breakdown voltage, high acoustic velocity and it can be

[1] To whom any correspondence should be addressed.

grown by reactive sputtering technique at relatively low temperature thus being compatible with CMOS device technology [3][4].

It is also becoming important to be able to integrate piezoelectric films with materials used in medical devices. Ultrananocrystalline diamond (UNCD) in thin film form, is a multifunctional material, which is extremely bioinert and biocompatible [5][6][7][8]; in addition, UNCD is capable of being integrated with CMOS technologies. For example, UNCD has been developed as an hermetic bioinert/biocompatible encapsulating coating for a Si-microchip [9] to enable implantation inside the eye on the retina, as a critical component of an artificial retina, and as a biocompatible coating for glaucoma valves [10] and dental implants [11].

Since both UNCD and AlN films can be processed via photolithography and reactive ion etching processes used in fabrication of Micro/Nanoelectromechanical Systems (NEMS), it has been shown that the integration of UNCD and AlN films provides the bases for developing a new generation of biocompatible Bio-MEMS/NEMS [12].

Because diamond-based substrates exhibit the highest sound velocity among all materials [13] and AlN exhibits the highest phase velocity among all piezoelectric materials [14], the AlN/diamond heterostructure provides a very promising platform for fabrication of a wide range of devices from SAW to microfluidics. Zalazar et al. [12], reported the integration of films on UNCD layers exhibiting a piezoelectric coefficient of about 5.3 pm/V, one of the highest for AlN film demonstrated today.

This work is focused on the development of an AlN/UNCD-based thin film bulk acoustic wave resonator for biomedical applications. In this case, a FBAR piezoelectric biosensor was fabricated and characterized. The device has been previously modelated and simulated under different conditions by the author [15]; even though it was carried out the analysis of the behaviour of a FBAR piezoelectric mass sensor, it can be extended to new types of sensor devices.

2. Geometry design

The simplest configuration of the membrane FBAR involves the acoustic resonance cavity formed by the creation of an air cavity underneath the resonating membrane by etching completely a Si substrate. To acoustically isolate the resonance cavity, parts of the substrate are removed to create a freestanding membrane. The membrane is composed of a Pt/Ti/AlN/Pt/Ti/UNCD multilayer on a silicon substrate as shown in the scheme of Figure 1a. Pt layers serve as bottom and top electrode to apply voltage to excite the piezoelectric effect on the AlN layer for actuation of the FBAR device. Top electrode (Pt/Ti) is similar to the bottom electrode.

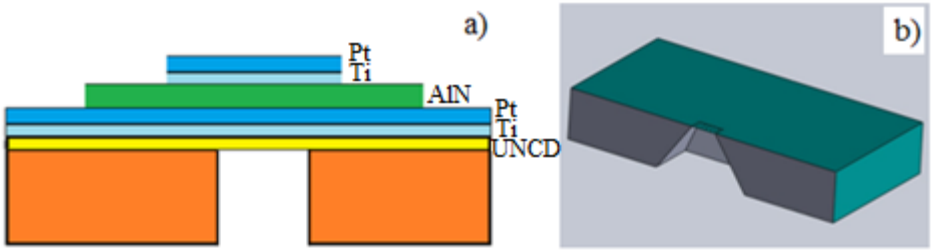

Figure 1. UNCD-based AlN FBAR. a) Scheme of the proposed heterostructure of Pt/Ti/AlN/Pt/Ti/UNCD/SiO2/Si and b) 3D longitudinal cut image of the freestanding FBAR heterostructure.

Devices composed of multilayer structures where the layers exhibit different thermal expansion coefficients often suffer from intrinsic residual stresses, which can be reduced using low temperature processes. In addition, being a low temperature process makes it promising for integrating with the IC technology.

An scheme of the FBAR device can be observed in Figure 1b. It can be seen a longitudinal cut of the freestanding heterostructure membrane composed by a Pt/Ti/AlN/Pt/Ti/UNCD multilayer on the silicon substrate.

3. Mask design and fabrication

The Layout Editor of the Tanner EDA software was used for the masks design. Layout is essentially a drawing process where the 2D drawings of the geometries will end up on the desired mask. Layout tools are essentially CAD (computer aided design) drawing tools, but include additional useful features.

Three different masks for the entire device were designed and fabricated:

- Mask 1: cavity on Si
- Mask 2: piezoelectric AlN
- Mask 3: top electrode

Figure 2 shows the mask for the cavity on the Si substrate. It can be observed the four different sizes used in this experimental step in order to compare their performances. Square membranes were designed for the FBARs.

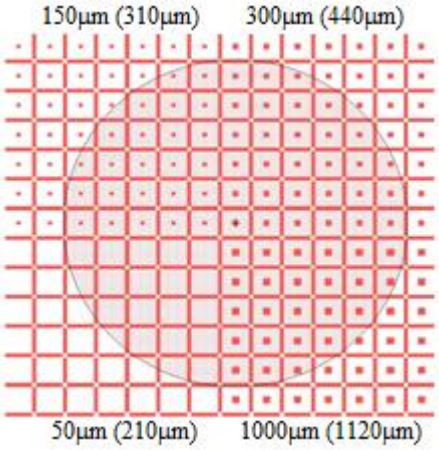

Figure 2. Mask layout for the Si cavity. It can be observed the four different sizes used in this experimental step, where the value in microns is the calculated length of the square while in brackets is the real length due to undercuts.

For the cavity design, the substrate material as well as the used etching method has to be considered. In the case of silicon, a common etching method is the wet anisotropic etching; potassium hydroxide (KOH) is an strong base capable of attack the Si substrate in an anisotropic way. N-type Si (100) wafers with surface polished to mirror finish as substrate were used, so the KOH will etch the Si preferably in the [100] plane. It produces the characteristic V anisotropic etch of the walls, forming an angle of 54.7° with respect to the main surface (Figure 3).

Figure 3. Si (100) showing characteristic V anisotropic etch of the walls forming an angle of 54.7° with respect to the main surface.

The used masks have a multilayer structure with the following layers: PR/Cr2O3/Cr/glass. The photoresist (PR) is the last layer and the Cr2O3 serves as antireflective film. The glass is highly flat and made of borosilicate glass. The fabrication of the masks was done by a Laser Pattern Generator (LW405). The pattern was generated over the photoresist on the chrome layer and the glass (square shape of 125 mm) during 24 hs. After that, the photoresist was developed (developer 351) and a wet etching of the chrome film was done.

4. FBAR fabrication

The freestanding membrane fabrication on the Si substrate involves several steps:

4.1 UNCD growth

A UNCD film on the front of the silicon wafer (N-type mirror polished Si (100)) was deposited. UNCD layers were grown using a MPCVD system (Lambda Technologies), powered by a 915 MHz magnetron generator with 2300 W power. It generates a plasma from a mixture of Ar (99%)/CH4 (1%) gases producing C2 dimers as the growth species at a pressure of 80mTorr. This layer was used as a substrate for the AlN and also serves as a stop layer for the anisotropic wet etching of the Si by using KOH.

4.2 Si3N4 mask

Silicon Nitride (Si3N4) was used as a mask for the wet etching of the Si using KOH. Commercial, polished, low stress Si3N4 residual (LSLPCVD, commercial grade, University wafer Inc) was used. Si3N4 pattern for the cavities was performed by photoresist spin coating (S1813), UV exposure for 5 seconds (mask aligner Karl Suss MA6), resist development (351 developer diluted in a 3: 1 ratio in DI water) and dry etching of the Si3N4 in a Tetrafluoromethane (CF4) plasma (Oxford CS-1701 RIE).

4.3 Pt/Ti deposition

The Pt layer was grown by magnetron sputter deposition on top of a Ti film deposited on the SiO2 surface as an adhesion layer. The Pt bottom electrode was grown by sputter deposition (AJA ATC Orion thin film deposition system). The Ti film provides an adhesion layer for growing highly c-axis (002) oriented AlN films. Films were deposited with a target RF power of 150W, pressure of 3 mTorr, Ar flow rate of 26sccm and base pressure of 1e-7 Torr. The thicknesses of the Platinum and Titanium were 150nm (720s deposition) and 10nm (310s deposition) respectively. In addition, this coating provides seeding capability and serves as a buffer layer, lowering the discrepancy in lattice parameter between substrate and film. It also helps to improve the adhesion of the AlN to the UNCD

4.4 AlN deposition

AlN films for MEMS devices are most often synthesized in the Wurtzite hexagonal crystallographic structure with c-axis (002) orientation perpendicular to the surface (diffraction peak at 36°), which is the orientation that yields the highest piezoelectric constant in addition to a high acoustic wave velocity [16].

AlN (002) oriented films were grown on the Pt layers at 500°C C at a pressure of 3mTorr, using reactive sputter deposition (AJA ATC Orion thin film deposition system), via sputtering material from an Al metallic target. Ar-plasma was used to produce Ar ions to sputter the Al material in a N2 atmosphere to produce the AlN films. Aluminum target with a diameter of 4" and a purity of 99.999% was used.

Several experiments were performed until reach to the crystallographic orientation (002) of the AlN with the diffraction peak in 36°. AlN layers with thickness in the 260-420 nm range were synthesized on silicon oxide (SiO2) and silicon nitride (Si3N4) were used as intermediate layer grown on Si.

4.5 AlN pattern

The pattern was transferred to the AlN film by spin coating of the photoresist (ma-N 415 negative photoresist), UV exposure for 30 seconds (mask aligner Karl Suss MA6), resist development (533) and dry etching using anisotropic Cl2-based reactive ion etching (Oxford CS-1701 RIE).

4.6 Electrode pattern

Patterning of Pt/Ti top electrode was done by applying lift off techniques. Firstly, a spin coating with S1813 on the frontside of the wafer, UV exposure and resist development were done. Finally a Pt/Ti sputter deposition and posterior removal of the photoresist was performed.

4.7 Cavity

The cavity etching was carried out on the backside by using KOH (30%). Hermetic protection to avoid frontside etching was used. Time etching was estimated in 9 hs at a temperature of 85°C using 250 rpm stirring.

The first cavity prototype can be seen in Figure 4, using only UNCD as membrane on the Si wafer substrate:

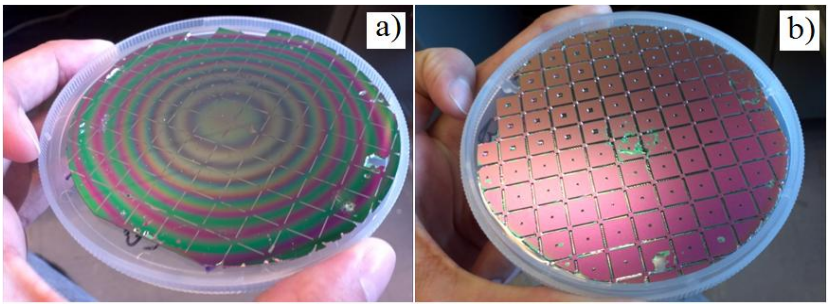

Figure 4. First cavity prototype. a) Frontside of the UNCD film and b) backside showing the different sizes of the cavities within dices.

5. Characterization

5.1 X-ray diffraction (XRD)

The XRD θ-2θ diffraction pattern taken from the XRD analysis of AlN/Pt/Ti/UNCD/SiO2/Si multilayer were scanned between 20° and 80°. Figure 2 shows an XRD θ-2θ scan of the AlN/Pt/Ti/UNCD/SiO2/Si layered film exhibiting high c-axis orientation for the AlN film. The presence of hexagonal AlN (002) diffraction peak at 36.05° can be noted, revealing the presence of mainly a (002) textured AlN film. Also, two Pt peaks, (111) at 40.05 and (002) at 46.5 are present. The weak peaks at 44.7 and at 65.1 correspond to Al (002) and Al (202), respectively. The strong narrow peak at 33.2 comes from the silicon wafer substrate and is the result of Si crystalline imperfections.

The X-ray wavelength was λ=1.540598A (Kα1, Long Fine focus, Cu Anode radiation). By using Bragg's law, it was calculated the c-lattice constant for the AlN layer. Its value was 4.9681 Å, which is in a good agreement with the value of the AlN found in the literature [17].

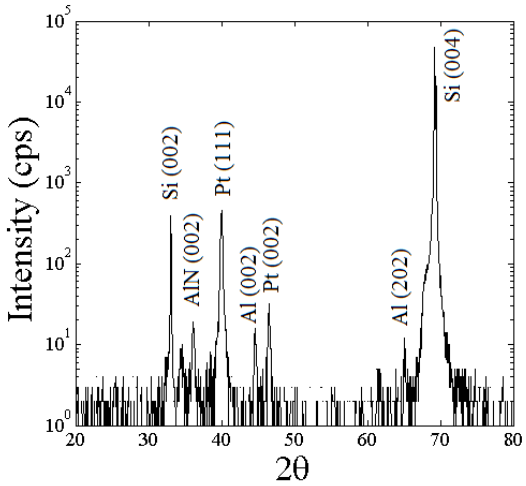

Figure 5. XRD spectrum of an AlN/Pt/Ti/UNCD/SiO2/Si heterostructure showing the characteristic peaks of the Pt layers and Si substrate, in addition to the critical AlN (002) peak that reveals the high orientation of AlN necessary to yield the high piezoelectric coefficient.

5.2 Optical Microscope

A fast analysis tool is the optical microscope. The obtained images help to evaluate the quality of the KOH etching. The morphology of the membranes and cavities are shown in Figure 6. The difference in the square membranes between frontside and backside of the Si wafer, was caused by the classical

pyramid shaped Si material; it obeys the preferential anisotropic etching direction (54.7°) of the (100) crystal plane of the Si wafer.

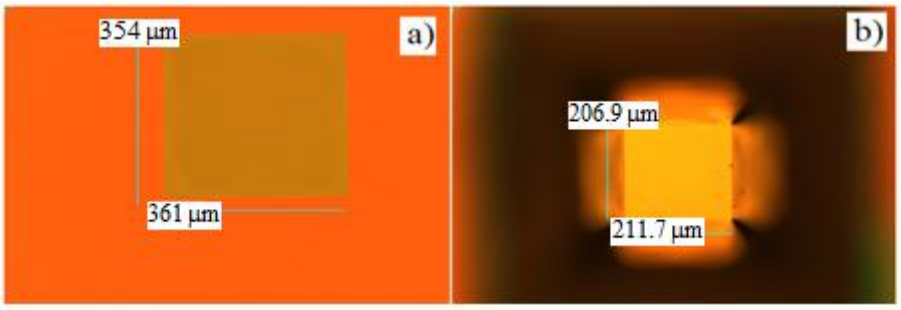

Figure 6. Square UNCD membranes. a) Membrane (mask 300 µm) seen from the frontside, and b) membrane (mask 150 µm) seen from the backside (cavity).

It can be seen that the size of each membrane is moderately higher than the expected due to the generated undercuts below the membranes. Undercuts increase the squares sizes in a range between 50-170 µm. The calculated etching rate for the Si using KOH was 1.16 µm/min

5.3 Scanning Electron Microscope

The scanning electron microscope (SEM) is a routinely used instrument for the examination of fine detail of a variety of samples. The instrument is, in simple terms, analogous to an optical microscope: the electron source (gun) is equivalent to the light source and the glass lens is replaced by electromagnetic lens. Information from the sample is collected and displayed on a viewing screen for visual interpretation.

In Figure 7a, a cross section of the AlN/Pt/Ti/UNCD membrane (cantilevered) is depicted. It exhibits a columnar microstructure. These columnar crystals are perpendicular to the substrate surface in agreement with the XRD results where the AlN film is highly textured. The piezoelectric film reached a thickness of 417nm after 5hs of growth thus arriving to a deposition rate of 83.4 nm/h (Figure 7b). This rate was affected by the low Ar flow used, reducing the amount of heavy ions impacting on the target. The UNCD layer used was 420 nm in thickness.

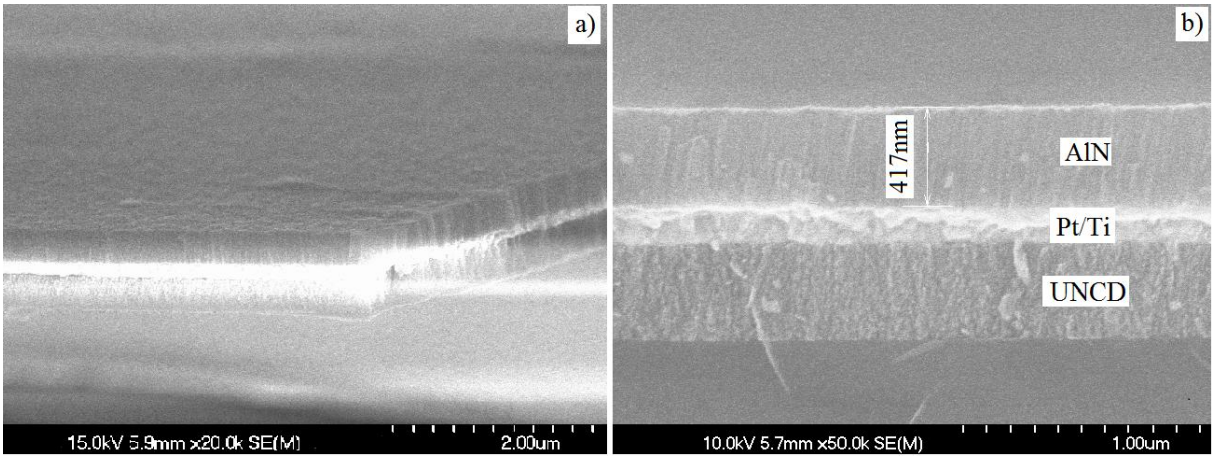

Figure 7. SEM cross section of the film for the AlN/Pt/Ti/UNCD membrane. a) Cantilevered membrane and b) measurements on the SEM image.

A clarified view of the generated Si cavity can be appreciated in the SEM image of the freestanding AlN/Pt/Ti/UNCD membrane on the Si substrate (Figure 8). It can be seen an in-focus image of the tilted Si walls (54.7°) where the big square have the dimensions of the mask and the smaller is the AlN/Pt/Ti/UNCD membrane. The white frame surrounding the big square is produced by the generated undercuts under the UNCD.

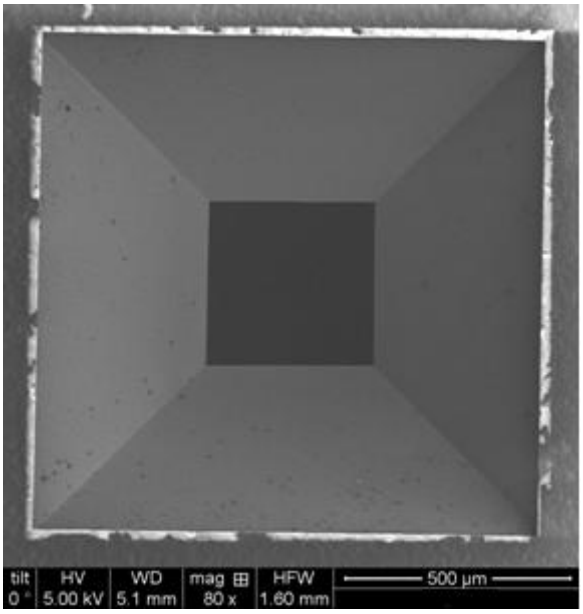

Figure 8. SEM image of the freestanding AlN/Pt/Ti/UNCD membrane on the Si substrate.

6. Conclusions

The feasibility of the fabrication of AlN/diamond-based FBAR structure has been demonstrated.

A direct method for the deposition of AlN on Pt/Ti/UNCD/SiO2/Si substrate avoiding polishing steps and thus reducing fabrication times has been demonstrated. It have been shown that thin AlN films with high (002) orientation can be produced

The columnar structure of the obtained AlN shows a highly textured film thus allowing the fabrication of FBAR resonators as well as piezoelectric actuators. The Pt film has proven to be a good buffer layer serving also as bottom and top electrodes.

Material compatibility with IC fabrication opens the way for monolithic integration of the traditionally incompatible IC and electro-acoustic technologies.

FBAR based on AlN/diamond materials is a very promising structure for biomedical applications. It is the opinion of the author that a huge field for biomedical devices based on AlN/UNCD is awaiting to be explored.

Acknowledgments

Authors thank the financial aid received by the Consejo Nacional de Investigaciones Científicas y Técnicas (CONICET), Argentina. Furthermore, authors thank the collaboration of Orlando Auciello and Pablo Gurman from the department of Materials Science and Engineering and Bioengineering, University of Texas at Dallas, USA.

References

[1] Chung K H, Liub G T, Duhb J G and Wang J H 2004 *Surface & Coatings Technology* pp 188-

189 745.
[2] Chen C C Lin C T Lee S Y Lin L H Huang C F and Ou K L 2007 *Applied Surface Science* 253, 5173.
[3] Chou C H Lin Y C Huang J HTai N H and Lin I 2006 *Diamond Relat. Mater*. 15, 404.
[4] Dubois M and Muralt P 1999 *Appl. Phys. Lett*. 74, 3032.
[5] Auciello O and Sumant A V 2010 *Diamond Relat. Mater*. 19, 699.
[6] Auciello O and Shi B 2010 *Biol. Med. Phys. Biomed.* 63.
[7] Bajaj P Akin D Gupta A Sherman D Shi B Auciello O and Bashir R 2007 *Biomed. Microdevices* 9, 787.
[8] Auciello O Birrell J Carlisle J A Gerbi J E Xiao X Peng B and Espinosa H D 2004 *J. Phys.: Condens. Matter* 16, 539.
[9] Xiao X Wang J Liu C Carlisle J A Mech B Greenberg R Guven D Freda R Humayun M S Weiland J and Auciello O 2006 *J. Biomed. Mater. Res. B Appl. Biomater.* 77B, 273.
[10] Zhou D D and Greenbaum E (Eds.) 2010, Implantable Neural Prostheses vols. 1 and 2 *Techniques and Engineering Approaches*, Springer (2010).
[11] Auciello O Gurman P Berra A Saravia M J and Zysler R Ch. 6, in *Diamond- Based Materials for Biomedical Applications*, ed Narayan R Woodhead Publishing Ltd, Cambridge, UK (in press, 2012).
[12] Zalazar M Gurman P Park J Kim D Hong S Stan L Divan R Czpalewski D and Auciello O 2013 *Appl. Phys. Lett.* 102, 104101.
[13] Assouar M B Elmazria O Kirsch P and Alnot P 2007 *J. Appl. Phys*. 101, 114507.
[14] Ishihara M Nakamura T Kokai F and Koga Y 2002 *Diamond Relat. Mater*. 11, 408.
[15] Zalazar M Guarnieri F 2010 *Mecánica Computacional*, vol XXIX, 6665-6684.
[16] Meinschen J Behme G Falk F Stafast H 1999 *Appl. Phys. A: Mater. Sci. Process*. 69, 673.
[17] Hirama K Taniyasu Y and Kasu M 2010 *Jpn. J. Appl. Phys.,* Part 1 49, 04DH01.